Specificity Determinants of Allosteric Modulation in the Neuronal Nicotinic Acetylcholine Receptor: a Fine Line between Inhibition and Potentiation

Laura C. Cesa, Colin A. Higgins, Steven R. Sando, Dennis W. Kuo, and Mark M. Levandoski

Department of Chemistry, Grinnell College, Grinnell, Iowa

Received September 21, 2011; accepted November 4, 2011

ABSTRACT

We are interested in the allosteric modulation of neuronal nicotinic acetylcholine receptors (nAChRs). We have postulated that the anthelmintic morantel (Mor) positively modulates (potentiates) rat $\alpha3\beta2$ receptors through a site located at the $\beta(+)/\alpha(-)$ interface that is homologous to the canonical agonist site (*J Neurosci* **29**:8734–8742, 2009). On this basis, we aimed to determine the site specificity by studying differences in modulation between $\alpha3\beta2$ and $\alpha4\beta2$ receptors. We also compared modulation by Mor with that of the related compound oxantel (Oxa). Whereas Mor and Oxa each potentiated $\alpha3\beta2$ receptors 2-fold at saturating acetylcholine (ACh) concentrations, Mor had no effect on $\alpha4\beta2$ receptors, and Oxa inhibited ACh-evoked responses. The inhibition was noncompetitive, but not due to open channel block. Furthermore, the nature and extent of modulation did not depend on subunit stoichiometry. We studied six positions at the $\alpha(-)$ interface that differ between $\alpha3$ and $\alpha4$. Two positions ($\alpha3$Ile57 and $\alpha3$Thr115) help mediate the effects of the modulators but do not seem to contribute to specificity. Mutations in two others ($\alpha3$Leu107 and $\alpha3$Ile117) yielded receptors with appreciable $\alpha4$-character; that is, Mor potentiation was reduced compared with wild-type $\alpha3\beta2$ control and Oxa inhibition was evident. A fifth position ($\alpha3$Glu113) was unique in that it discriminated between the two compounds, showing no change in Mor potentiation from control but substantial Oxa inhibition. Our work has implications for rational drug design for nicotinic receptors and sheds light on mechanisms of allosteric modulation in nAChRs, especially the subtle differences between potentiation and inhibition.

Introduction

The neuronal nicotinic acetylcholine receptors (nAChRs) are a diverse family of ligand-gated ion channels and are members of the Cys-loop superfamily. They are implicated in neurological disorders such as Alzheimer's and Parkinson's diseases (Albuquerque et al., 2009). Perhaps more importantly, nAChRs have a central role in nicotine abuse, because nicotine increases the activation of reward pathways (Dani and Bertrand, 2007). The clinical successes of drugs such as varenicline for smoking cessation (e.g., Gonzales et al., 2006) and galanthamine in reducing cognitive impairments associated with Alzheimer's (Birks, 2006) suggest promise for pharmacological interventions tar-geting central cholinergic systems. Although nAChRs containing $\alpha7$ or $\alpha4/\beta2$ subunits have been a focus of drug development, specific roles for nAChRs in physiological processes and well defined nAChR subtypes remain unclear (e.g., Gotti et al., 2009); thus, the search for new nAChR ligands is still broad (Jensen et al., 2005).

Substantial recent interest has focused on allosteric modulators of nAChRs (Bertrand and Gopalakrishnan, 2007). Such compounds enhance or inhibit channel activity from binding sites that are noncompetitive with the canonical (orthosteric) agonist site. Some positive modulators have the advantageous property of being at most weak partial agonists. Thus, their potentiation of responses elicited by endogenous ACh may allow for temporal and spatial coincidence activation in cholinergic pathways, thereby avoiding the tonic activation expected for drugs that are full agonists (Maelicke and Albuquerque, 2000).

Several novel compounds and their allosteric modulatory effects have been reported. Examples include *N*-(5-chloro-2,4-

ABBREVIATIONS: nAChR, nicotinic acetylcholine receptor; PNU-120596, *N*-(5-chloro-2,4-dimethoxyphenyl)-*N*′-(5-methyl-3-isoxazolyl)-urea; LY-2087101, [2-[(4-fluorophenyl)amino]-4-methyl-5-thiazolyl]-3-thienylmethanone; MTS, methanethiosulfonate; OR2, oocyte Ringer's medium; Mor, morantel; Oxa, oxantel; Pyr, pyrantel.

dimethoxyphenyl)-N'-(5-methyl-3-isoxazolyl)-urea (PNU-120596) (Hurst et al., 2005) acting on $\alpha7$ receptors, KAB-18 (Henderson et al., 2010) acting on $\alpha4\beta2$ receptors, and [2-[(4-fluorophenyl)amino]-4-methyl-5-thiazolyl]-3-thienylmethanone (LY-2087101) with a less selective profile (Broad et al., 2006). In addition, a variety of previously known compounds act as allosteric modulators, such as the antiacetylcholinesterases galanthamine and physostigmine (e.g., Schrattenholz et al., 1996) and the anthelmintic ivermectin (Krause et al., 1998). We and others have shown that other anthelmintic compounds that are full agonists in lower species, causing spastic paralysis in the worm, also allosterically potentiate human and rat nAChRs (e.g., Bartos et al., 2006; Wu et al., 2008).

Localizing ligand binding sites is of primary concern for a complete understanding of allosteric modulators—and is crucial for any rational drug design efforts. The identification and elaboration of the canonical agonist and competitive antagonist binding site at the $\alpha(+)$/non-$\alpha(-)$ interface of the receptor extracellular domain is a well developed aspect of the nAChR field (Arias, 2000; Sine and Engel, 2006). Work based on X-ray crystal structures of the nAChR extracellular domain homolog acetylcholine binding protein, as well as a model of the entire muscle-type receptor and homology modeling thereof, has enriched our understanding of receptor-ligand interactions (e.g., Rucktooa et al., 2009). This information is now being employed to determine binding sites for allosteric modulators of nAChRs (e.g., Nirthanan et al., 2008; Collins and Millar, 2010). Although technical limitations and subtype diversity together currently preclude an atomic-resolution picture of many neuronal nAChR systems of interest, the available models still have very strong predictive power in guiding structure-function studies of nAChRs.

On the basis of our studies of anthelmintics as allosteric modulators, we proposed as a general feature of the receptors that nAChR ligand "pseudo-sites" occur at the noncanonical subunit interfaces [e.g., $\beta(+)/\alpha(-)$ for morantel (Mor); Seo et al. (2009)]. From this premise, several important questions about the nature of these sites arise: which features are common to both canonical and noncanonical sites, thus constituting a generalized nAChR ligand site, and which features differentiate canonical (agonist/competitive antagonist) from noncanonical (modulator) sites? What are the determinants of specificity for allosteric modulators acting on different receptor subtypes? Such questions seem of increasing importance given the recent demonstration that the $\alpha(+)/\alpha(-)$ interface in $(\alpha4)_3(\beta2)_2$ receptors constitutes a low-sensitivity agonist site (Harpsøe et al., 2011; Mazzaferro et al., 2011). The answers to such questions are one of the keys to the development of therapeutic agents against neuropathologic conditions involving nicotinic receptors. In this study, we identify the determinants of specificity of the $\beta2(+)/\alpha3(-)$ modulator site and discover that modulation can be interconverted between potentiation and inhibition by point mutations.

Materials and Methods

Reagents. All chemicals used, unless otherwise noted, were reagent grade and obtained from Sigma-Aldrich (St. Louis, MO). Morantel is 1,4,5,6-tetrahydro-1-methyl-2-(2-[3-methyl-2-thienyl]ethenyl)pyrimidine, tartrate salt. Oxantel is 1-methyl-2-(3-hydroxyphenylethenyl)-1,4,5,6-tetrahydropyrimidine, with 4,4′-methylenebis(3-hydroxy-2-naphthoic acid). Pyrantel is 1-methyl-2-(2-[2-thienyl]ethenyl)-1,4,5,6-tetrahydropy-

rimidine, with tartrate salt. Methanethiosulfonate (MTS) reagents were purchased from Toronto Research Chemicals (Toronto, ON, Canada). Those used in this study were [2-(trimethylammonium)ethyl]-methanethiosulfonate and imidazole 4-methyl methanethiosulfonate.

Nicotinic Receptor Clones and Mutagenesis. Plasmids of the pGEMHE background bearing wild-type rat $\alpha3$ and $\beta2$ cDNA sequences were a gift from Dr. Charles Luetje (Miami University, Miami, FL); the clones were originally isolated in the lab of Dr. Jim Patrick (Baylor College of Medicine, Houston, TX) (Boulter et al., 1987). Mutant genes were created either by 1) the QuikChange temperature cycling method (Stratagene, La Jolla, CA) with complementary primers harboring the mutation or 2) custom mutagenesis from GenScript (Piscataway, NJ). Mutations were verified by complete sequencing of the entire extracellular domain region using capillary electrophoresis of dye-detected, dideoxy-generated fragments. Unless otherwise noted in the context of another receptor subtype, all $\alpha3$ and $\beta2$ residue numbering follows that in the structure a3b2rr.pdb (http://www.ebi.ac.uk/compneur-srv/LGICdb/HTML/a3b2rr.html) (Sallette et al., 2004); these position numbers are smaller by two compared with numbering used elsewhere in the literature; this discrepancy has arisen because of homology modeling based on a crystal structure of a protein of different sequence. The cDNAs were linearized with a unique restriction enzyme, and then were made RNase-free by phenol-chloroform extraction. RNAs were synthesized from these cDNAs using the T7 kit from Ambion (Austin, TX). RNAs were diluted with RNase-free water to 0.5 $\mu g/\mu l$ and stored at $-20°C$.

Oocyte Preparation and Injection. Functional receptors were expressed in *Xenopus laevis* oocytes harvested from oocyte-positive female frogs or whole ovary tissue (Nasco, Ft. Atkinson, WI) using procedures approved by the Grinnell College Institutional Animal Care and Use Committee in accord with the National Institutes of Health guidelines. In brief, stage V to VI oocytes were prepared by collagenase treatment and manual selection. Oocytes were maintained at 16°C in Barth's medium (88 mM NaCl, 1.0 mM KCl, 2.5 mM NaHCO$_3$, 0.30 mM Ca(NO$_3$)$_2$, 0.41 mM CaCl$_2$, 0.82 mM MgSO$_4$, 15 mM HEPES, and 2.5 mM sodium pyruvate, pH 7.6, supplemented with 100 U/ml penicillin/streptomycin and 50 μg/ml gentamicin). With the use of a Nanoject microinjector (Drummond, Broomall, PA), each oocyte was injected with 46 nl of a 1:1 (v/v) combination of the desired α and β subunits, prepared from 0.5 $\mu g/\mu l$ stock solutions. In a subset of experiments, 10:1 or 1:10 combinations (v/v; total of 46 nl per oocyte) were injected in accordance with previous work (Zwart and Vijverberg, 1998; Moroni et al., 2008). Allowing 2 to 4 days for receptor expression, with daily changes of Barth's medium and removal of dead cells, currents could be recorded for up to 7 subsequent days. Expression for all mutants was comparable with that for the wild-type $\alpha3\beta2$ and $\alpha4\beta2$ receptors as judged by currents in the range 0.2 to 4 μA evoked with a saturating ACh concentration (3 mM); expression seemed to depend more on the donor/injection batch than on subtype. Likewise, current traces for all mutants, including the triple and quintuple combinations, were very similar to those of wild-type $\alpha3\beta2$ (and not $\alpha4\beta2$; see Fig. 1A) at the same effective concentrations; this observation suggests that neither the mutations nor the modulators greatly affected the desensitization properties of the receptors, consistent with our previous results (Wu et al., 2008).

Macroscopic Current Recordings. Electrophysiology recordings were made with a Gene Clamp 500B amplifier (Molecular Devices, Sunnyvale, CA) to measure evoked currents from oocytes using the two-electrode voltage-clamp method, according to previous work (Wu et al., 2008; Seo et al., 2009). Voltage was clamped at -60 mV, with leak currents <200 nA, although larger leak currents were occasionally tolerated in the presence of a stable baseline. Perfusion and drug administration were controlled with solenoid valve systems (VC-6; Warner Instruments, Hamden, CT). Recording electrodes were filled with 3 M KCl and selected for resistances between 0.5 and 5 MΩ. Each oocyte was perfused with drug for 5 s and washed with oocyte Ringer's medium (OR2; 115 mM NaCl, 2.5 mM KCl, 1.8 mM

A
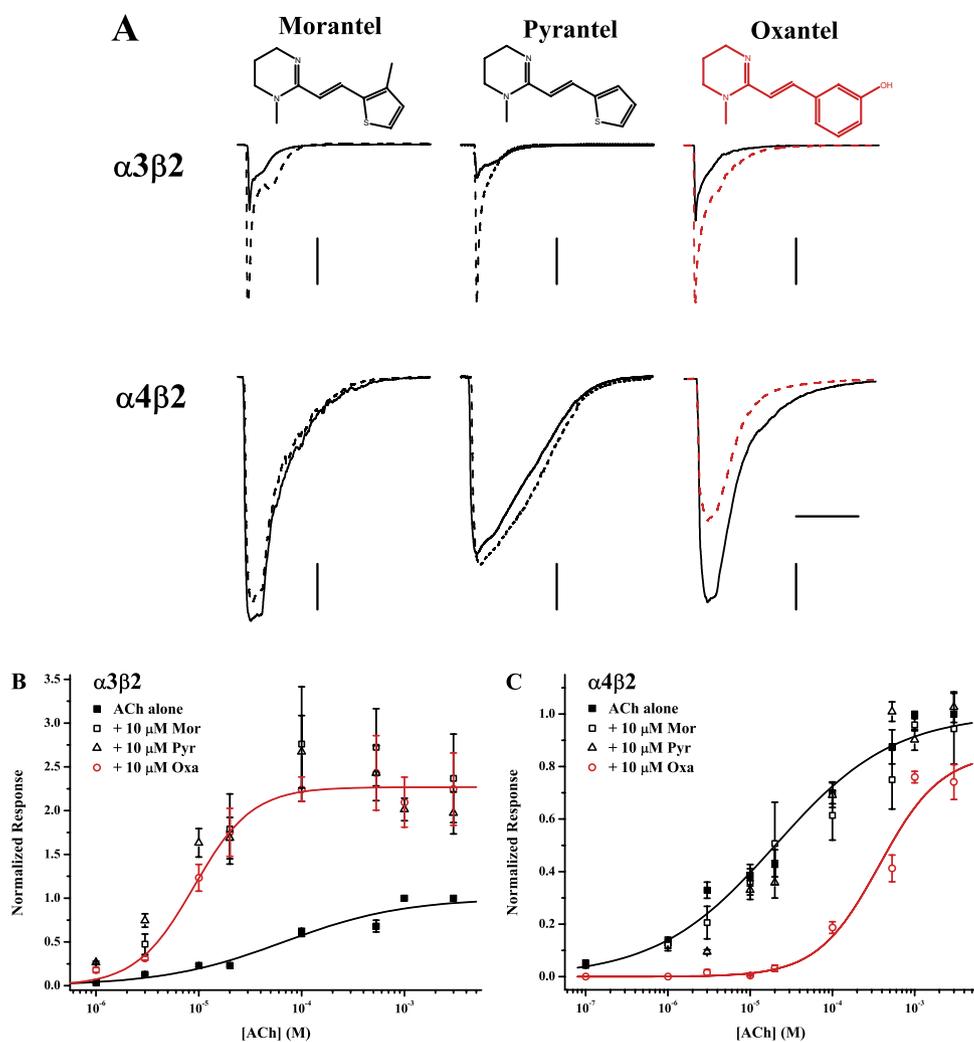
Fig. 1. Differential modulation by three anthelmintic compounds depends on the α subunit. A, representative traces for responses evoked by ACh and ACh + modulators are shown for oocytes expressing wild-type $\alpha 3\beta 2$ (top row) or wild-type $\alpha 4\beta 2$ receptors (bottom row). In each case, the control response to 100 μM ACh is shown as a solid trace and the response to 100 μM ACh + 10 μM modulator is overlaid as a dashed trace; the red traces for the Oxa-added condition highlight the differences in potentiation ($\alpha 3\beta 2$) versus inhibition ($\alpha 4\beta 2$). Horizontal scale bar, 20 s (applies to all experiments); vertical scale bar, 1.0 μA [except for $\alpha 3\beta 2$/pyrantel (0.4 μA), $\alpha 4\beta 2$/morantel (0.5 μA), and $\alpha 4\beta 2$/pyrantel (0.2 μA)]. B and C, the effects of the three anthelmintic compounds as a function of ACh concentration are displayed for wild-type $\alpha 3\beta 2$ (B) and wild-type $\alpha 4\beta 2$ receptors (C). Responses evoked by ACh alone are shown as ■, whereas responses to ACh + 10 μM modulator are given as □ (Mor), △ (Pyr), or red ○ (Oxa). All currents were normalized to the response to 3 mM ACh; values plotted are means ± S.E.M. Solid curves represent best fits of the Hill equation to the data sets. For clarity, only fits for ACh alone (black) and Oxa-added (red) are shown. Control ACh responses were collected separately for each experiment, but these were then analyzed in aggregate. Replicates were n = 3–12. Fits for the Pyr-added experiments not reported elsewhere were EC$_{50}$, 5.5 ± 1.7 μM; n_{H}, 1.24 ± 0.42; E_{max}, 2.8 ± 0.1 ($\alpha 3\beta 2$) and EC$_{50}$, 40 ± 10 μM; n_{H}, 0.78 ± 0.17; E_{max}, 1.1 ± 0.1 ($\alpha 4\beta 2$). See Table 1 for the parameters of other fits.

CaCl$_2$, and 10 mM HEPES, pH 7.3) for at least 90 s. Dilute drug solutions were prepared in OR2 from concentrated stocks. We determined spectrophotometrically that oxantel (Oxa) is fully soluble to at least 1 mM, which is consistent with the much higher calculated maximum solubility of 0.47 M under similar conditions [*SciFinder*; Chemical Abstracts Service: Columbus, OH, 2011; RN 58-08-2 (accessed October 20, 2011); calculated using ACD/Labs software, version 8.14; ACD/Labs 1994–2011]. Both of these exceed the highest concentration used in our experiments (300 μM). In experiments using MTS reagents, we followed established procedures (Karlin and Akabas, 1998); small aliquots of the crystalline reagent were dissolved in water and kept on ice before diluting to the working concentration in OR2 immediately before use in the experiment. Changes in current with respect to the baseline in response to the administration of drug were recorded. Current responses were recorded using Clampex 9.2 and measured with Clampfit 9.2 (Molecular Devices).

Concentration-response behavior for wild-type and mutant receptor subtypes, as well as potentiation for ACh plus modulator [Mor, Oxa, pyrantel (Pyr)] was characterized across the micromolar to millimolar range. Comparisons were made by fitting the Hill equation (fractional response = $E_{\mathrm{max}}/\{1 + (\mathrm{EC}_{50}/[\mathrm{agonist}])n_{\mathrm{H}}\}$) to concentration-response data for wild-type and mutant receptor subtypes; for all experiments testing modulators, currents were normalized to the response evoked by a saturating ACh concentration alone as an internal control. The ACh responses of the two wild-type subunit combinations (Fig. 1 and Table 1) were consistent with those in previous reports (Cohen et al., 1995; Hsiao et al., 2006). Unless

indicated otherwise, modulation was measured via coapplication of 10 μM modulator and ACh. Repeat measurements for the same oocyte were averaged, and responses for multiple oocytes were normalized as appropriate to the experiment (described in figure legends). Data are reported as means ± S.E.M.

Results

We are interested in a class of anthelmintic compounds that includes morantel, pyrantel, and oxantel (structures in Fig. 1A) as a model of allosteric modulation of neuronal nicotinic acetylcholine receptors (nAChRs). Having previously determined that Mor potentiation was quite specific for $\alpha 3\beta 2$ receptors (both rat and human; Wu et al., 2008), we carried out a limited structure-activity relationship study with these three anthelmintics. The two key results from this approach are demonstrated by the representative traces shown in Fig. 1A. First, whereas Mor and Pyr potentiated ACh-evoked currents for $\alpha 3\beta 2$ receptors, there was little to no effect of these compounds on $\alpha 4\beta 2$ receptors when coapplied with ACh. Second, although Oxa potentiated $\alpha 3\beta 2$ responses in the same manner as Mor and Pyr, it inhibited $\alpha 4\beta 2$ ACh-evoked currents.

Because the degree of potentiation is a strong function of both agonist and modulator concentration (Wu et al., 2008), we explored the full concentration-response behavior for the

TABLE 1

Agonist and modulator evoked response characteristics

The values in square brackets indicate the number of replicate oocytes for each measurement. Fits to the Hill equation for experiments with ACh + 10 μM Mor or ACh + 10 μM Oxa in all cases, except for α3L107Hβ2, which was ACh + 50 μM Oxa.

| Subtype | ACh Response | | Modulation Response | | | | | |
| | | | Mor | | | Oxa | | |
	EC$_{50}$	n_H [n]	EC$_{50}$	n_H	E_{max} [n]	EC$_{50}$	n_H	E_{max} [n]
	μM		μM			μM		
α3β2	66 ± 9	0.75 ± 0.07 [5–11]	10 ± 6	1.37 ± 0.80	2.64 ± 0.29 [5]	9 ± 1	1.54 ± 0.25	2.27 ± 0.06 [3]
α4β2	21 ± 4	0.59 ± 0.06 [6–12]	41 ± 9	0.49 ± 0.06	1.06 ± 0.14 [3–10]	370 ± 65	1.15 ± 0.36	0.85 ± 0.13 [5]
α3W53Aβ2	42 ± 2	1.08 ± 0.06 [6–10]	20 ± 3	1.28 ± 0.25	1.12 ± 0.04 [4]	47 ± 7	1.54 ± 0.24	1.16 ± 0.04 [4]
α3β2W149A	40 ± 6	0.99 ± 0.12 [5]	44 ± 6	1.38 ± 0.19	0.86 ± 0.03 [5]	110 ± 3	1.44 ± 0.06	0.90 ± 0.01 [6]
α3K109Fβ2	86 ± 14	0.66 ± 0.07 [12]	7 ± 2	1.13 ± 0.25	4.55 ± 0.22 [7]	13 ± 3	1.45 ± 0.46	3.53 ± 0.19 [5]
α3L107Cβ2	62 ± 7	0.71 ± 0.06 [6–9]	4.9 ± 0.9	1.33 ± 0.33	3.49 ± 0.15 [3]	13 ± 2	1.11 ± 0.13	1.56 ± 0.04 [7]
α3L107Hβ2	27 ± 4	1.02 ± 0.13 [17]	18 ± 2	1.15 ± 0.13	1.15 ± 0.03 [9]	106 ± 9	2.21 ± 0.78	1.04 ± 0.04 [8]
α3E113Rβ2	40 ± 5	1.01 ± 0.12 [10]	10 ± 6	1.53 ± 0.95	2.03 ± 0.22 [5]	80 ± 8	1.59 ± 0.24	0.97 ± 0.03 [5]
α3T115Cβ2	120 ± 20	0.71 ± 0.07 [9]	5 ± 2	1.48 ± 0.79	2.84 ± 0.22 [5]	9 ± 2	0.96 ± 0.21	1.62 ± 0.08 [4]
α3T115Qβ2	280 ± 40	0.96 ± 0.12 [5–10]	2.2 ± 0.6	1.27 ± 0.49	5.14 ± 0.29 [5]	18 ± 3	2.23 ± 0.75	5.03 ± 0.23 [5]
α3I117Tβ2	16 ± 2	0.93 ± 0.08 [15]	37 ± 12	0.85 ± 0.19	0.97 ± 0.07 [8]	50 ± 7	1.24 ± 0.17	0.95 ± 0.03 [7]
α3I57Eβ2	110 ± 10	0.83 ± 0.05 [5–13]	6 ± 3	0.57 ± 0.23	1.70 ± 0.17 [7]	6 ± 2	0.90 ± 0.25	1.15 ± 0.06 [6]
α3/α4[3]β2	22 ± 4	0.93 ± 0.13 [9]	26 ± 8	1.06 ± 0.32	0.94 ± 0.07 [4]	59 ± 18	1.50 ± 0.53	0.47 ± 0.04 [5]
α3/α4[5]β2	20 ± 3	1.15 ± 0.19 [10]	18 ± 5	1.31 ± 0.43	0.93 ± 0.05 [4]	94 ± 13	0.95 ± 0.11	0.88 ± 0.03 [6]

three anthelmintics on both α3β2 and α4β2 nAChRs. As shown in Fig. 1B, the three compounds potentiated ACh-evoked currents in a quantitatively indistinguishable manner; each of the three parameters characterizing the Hill equation fits are the same within error across the three drugs (see Table 1 and the legend to Fig. 1). It is noteworthy that these compounds potentiated at saturating concentrations of agonist (I$_{+modulator}$/I$_{control}$ ~2.3), a macroscopic indication of increased efficacy of channel gating (Wu et al., 2008).

In contrast, Mor and Pyr failed to potentiate α4β2 responses (Fig. 1C); Hill equation fits for the modulator-added condition are indistinguishable from their matched-pair ACh-alone controls (Table 1; Fig. 1 legend). We were surprised to find that 10 μM Oxa inhibited all ACh-evoked currents across this range, with an 18-fold decrease in potency for the evoked response. The increased Hill slope and decreased maximum response (at the highest ACh concentrations) are immediate indications that Oxa inhibits α4β2 receptors noncompetitively (Rang, 1981; Colquhoun, 1998). In addition to the fit to the entire data set denoting a decreased efficacy (E_{max} = 0.85 ± 0.13), the ACh + Oxa responses at 1 and 3 mM ACh were significantly smaller than those of controls (t test; $p < 0.05$). At this level of analysis, Mor and Pyr had identical behavior; we therefore focused only on identifying the origins of the differences between Mor and Oxa.

We next investigated in more detail the mechanism of Oxa inhibition of α4β2 responses. Figure 2A demonstrates that, although inhibition of ACh-evoked currents increased with increasing Oxa concentration, the currents could not be com-

pletely eliminated under these conditions (100 μM ACh ~EC$_{70}$), as would be expected for competitive inhibition. This incomplete inhibition is unlikely to arise from Oxa insolubility, because the highest concentrations we used are well below the maximum solubility under these conditions (see *Materials and Methods*). Many nAChR ligands are positively charged and inhibited by an open channel blocking mechanism at high concentration (Buisson and Bertrand, 1998; Arias et al., 2006). We therefore measured Oxa inhibition of α4β2 as a function of membrane holding potential. As can be seen in Fig. 2B, Oxa inhibition was not strongly voltage-dependent and, if anything, showed a slight increase as the cell was depolarized. This behavior is opposite that expected for an open channel blocker, the inhibition by which becomes more severe at hyperpolarized potentials because of the increased driving force to cross the membrane (Buisson and Bertrand, 1998). Note also that the degree of inhibition was greater for the lower (100 μM) ACh concentration at all potentials measured; this behavior is also opposite that expected for competitive and open channel block mechanisms (Rang, 1981).

Numerous studies have demonstrated that the stoichiometry of α4 and β2 subunits in heterologously expressed receptors dictates their response to agonists and antagonists, as well as allosteric modulators (e.g., Zwart and Vijverberg, 1998; Moroni et al., 2008). We therefore measured Oxa inhibition of α4β2 receptors as a function of the ratio of the subunit RNAs injected, in accordance with the previous work cited above in choosing the ratios 10:1 and 1:10. Figure 2C shows that Oxa inhibition is substantial throughout the
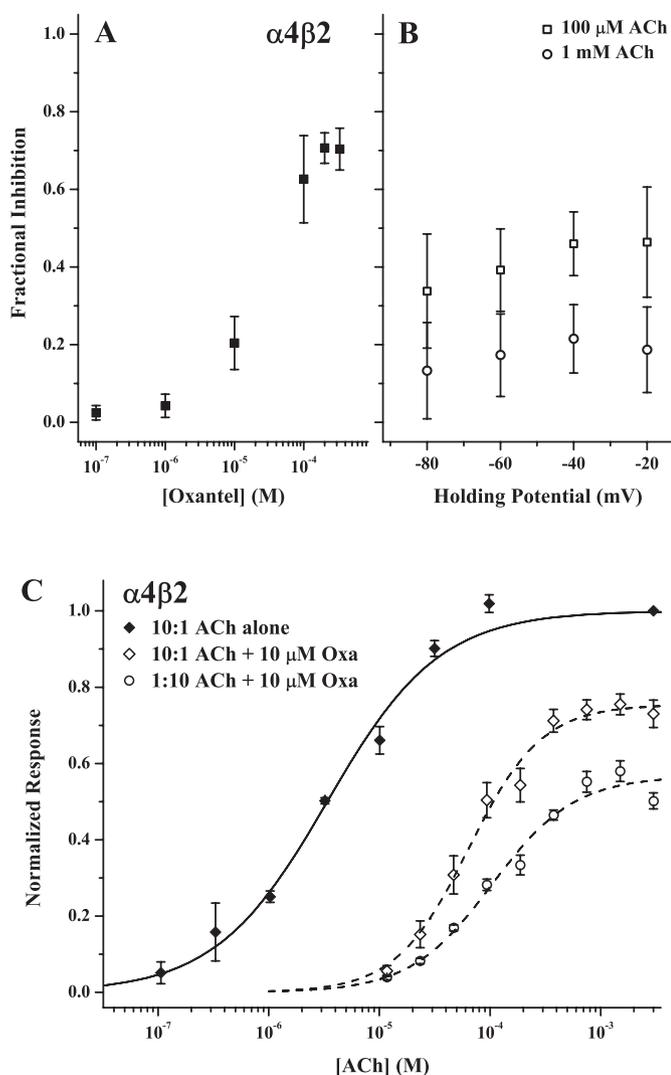
Fig. 2. Oxantel inhibition is noncompetitive and independent of subunit stoichiometry. A, fractional degree of inhibition by Oxa [($I_{ACh} - I_{ACh+Oxa}$)/I_{ACh}] as a function of Oxa concentration. The control, uninhibited response was elicited with 100 μM ACh with the holding potential at -60 mV. B, data for a separate experiment to determine the voltage-dependence of Oxa inhibition. Currents were evoked with two ACh concentrations (100 μM and 1 mM) and inhibition by coapplication was measured. Symbols represent means $\pm$ S.E.M. for $n = 4$ oocytes for both experiments. C shows concentration-response data for ACh alone ($\blacklozenge$) and in the presence of 10 μM Oxa ($\lozenge$) for oocytes injected with RNA ratios of 10:1 $\alpha 4$:$\beta 2$, and for ACh + 10 μM Oxa for oocytes injected with 1:10 $\alpha 4$:$\beta 2$ ($\bigcirc$). Symbols represent mean currents normalized to the response evoked by 3 mM ACh alone ($\pm$ S.E.M.). Curves represent best fits of the Hill equation to the data. The parameters not reported elsewhere were EC_{50}, 64 $\pm$ 7 μM; n_H, 1.32 $\pm$ 0.17; E_{max}, 0.75 $\pm$ 0.02 (dashed curve, Oxa inhibition for 10:1 ratio) and EC_{50}, 105 $\pm$ 12 μM; n_H, 1.17 $\pm$ 0.13; E_{max}, 0.57 $\pm$ 0.02 (dashed curve, Oxa inhibition for 1:10 ratio); EC_{50}, 9.2 $\pm$ 0.8 μM; n_H, 0.75 $\pm$ 0.05 (ACh control for 10:1 ratio, omitted for clarity) and EC_{50}, 3.4 $\pm$ 0.4 μM; n_H, 0.86 $\pm$ 0.07 (solid curve, ACh control for 1:10 ratio). The replicates were $n = 3$ (ACh alone) and $n = 4$ and 5 (Oxa inhibition).

range of ACh concentrations tested, including at saturation ($\sim$1 mM). Comparison with Fig. 1C reveals that Oxa inhibition of the 10:1 and 1:10 combinations is qualitatively the same as the 1:1 subunit RNA ratio. Furthermore, we obtained the same result (equivalent Oxa inhibition) when we coexpressed wild-type $\alpha 4$ with the $\beta 2(+)$ mutant β2T150C in 10:1 and 1:10 ratios (data not shown). Although the degree of inhibition of the 10:1 and 1:10 $\alpha 4$:$\beta 2$ combinations may differ
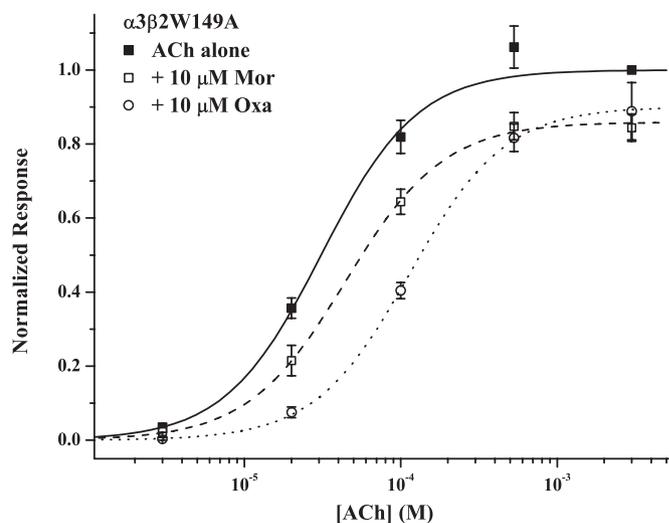

Fig. 3. A role for tryptophans in modulation. The effects of Mor and Oxa on the concentration-response behavior of mutant $\alpha 3\beta$2W149A receptors are shown. The two experiments (as five-point ACh $\pm$ modulator titrations) were collected separately, each with the series of control ACh responses, but the controls were then analyzed in aggregate. Symbols represent mean currents normalized to 3 mM ACh alone ($\pm$ S.E.M.), and fits of the Hill equation are reported in Table 1. The replicates were $n = 5$ (+ Mor, $\square$ and dashed curve), $n = 6$ (+ Oxa, $\bigcirc$ and dotted curve), and $n = 11$ (ACh controls, $\blacksquare$ and solid curve).

slightly from one another and from the 1:1 ratio, these results suggest that both α and β subunits are necessary for the effect (see also below) and that the different modes of modulation by Mor and Oxa do not arise because each compound acts preferentially on a receptor isoform of different stoichiometry.

Chemical modification studies of a series of cysteine-substituted residues provided evidence that Mor binds in the $\beta(+)/\alpha(-)$ interface, in a pocket structurally homologous to the canonical/agonist binding site (Seo et al., 2009). In particular, both tryptophans and two of the three tyrosines of the so-called aromatic box (Arias, 2000; Sine and Engel, 2006) are conserved in this interface. We therefore sought to substantiate that tryptophans 149 of $\beta 2$ and 53 of $\alpha 3$ (see Fig. 4) play a role in allosteric modulation by these anthelmintics. As shown in Fig. 3, the concentration-response experiments for $\alpha 3\beta$2W149A receptors support this idea. In contrast to the very large degree of potentiation by Mor and Oxa on wild-type $\alpha 3\beta 2$ receptors, both modulators gave mild inhibition of the ACh response. We found nearly identical results with the α3W53A$\beta 2$ mutant (Table 1). It is noteworthy that both tryptophan-to-alanine mutants responded to ACh just as well as wild-type receptors (each has slightly larger n_H; Table 1), indicating that the loss of Mor and Oxa potentiation does not arise from a general impairment of receptor function.

Given this further support for a modulator binding site located near, and possibly involving, β2Trp149 and α3Trp53, we turned our attention to elucidating the specificity differences between $\alpha 3$- and $\alpha 4$-containing receptors and between Mor and Oxa. Figure 4 shows a homology structural model of the $\beta(+)/\alpha(-)$ interface (Sallette et al., 2004), based on the acetylcholine binding protein X-ray crystal structure (Brejc et al., 2001), and an alignment of the rat $\alpha 3$ and $\alpha 4$ sequences for the equivalent of loops D and E from the canonical binding site. We reasoned that residues differing in the two subunits give rise to the specificity differences; those we selected for study are color-coded with the side chains shown in the
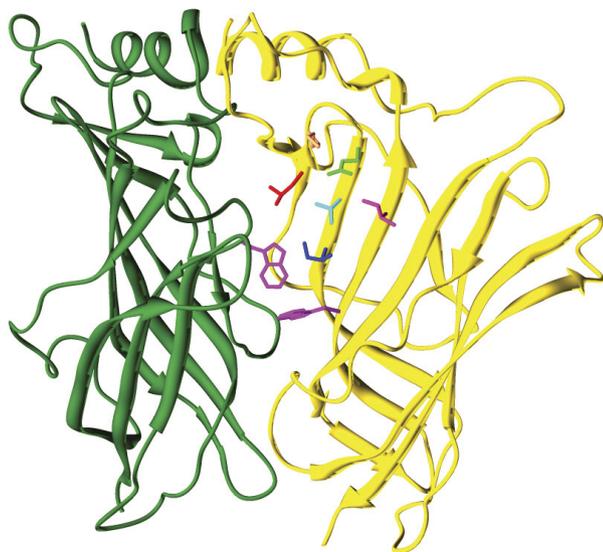
	53	57	107	113	117
α3	WLKQ**I**WNDY		KA**L**L**K**YTG**E**V**T**W**I**P		
α4	WVKQEWHDY		KAHLFYDGRVQWTP		

Fig. 4. The noncanonical interfaces of α3β2 and α4β2 diverge. A homology model of the extracellular domain β2(+)/α3(−) interface is shown in ribbon format; β2 (left) is green and α3 (right) is gold. The tryptophan side chains (magenta; Trp149 of β2 and Trp53 of α3) conserved in the canonical/agonist binding site are shown in stick format. Below the structure is an alignment of the rat α3 and α4 sequences in the regions of the D and E loops. The side chains (stick format) chosen for specificity studies are color-coded in the α3 sequence; numbering is for the mature α3 protein. This depiction is derived from a3b2rr.pdb (Sallette et al., 2004).

structure (Fig. 4). Note that the residues differing between α3 and α4 alternate with residues identical in the two, and that these identical amino acids are largely hydrophobic in character. This observation is consistent with the structural prediction that these stretches form β-strands with the hydrophobic residues directed toward the interior and that the alternating residues constitute diverse surfaces in this region for the two subunits (compare Teissére and Czajkowski, 2001).

Figure 5 illustrates the effects of substituting α4 residues into the α3 subunit for three of the six positions we examined. For the mutants α3L107H, α3E113R, and α3I117T (Fig. 5, A–C, respectively), the ACh-control concentration-response behavior was quite similar to that for wild-type α3β2 (see Table 1), although the parameters trended toward the α4 behavior. Again, these results indicate that the mutations do not significantly disrupt receptor function. In contrast to the wild-type–like ACh activation for these three mutants, each had a different pattern of response for Mor and Oxa modulation.

Mor potentiation was markedly reduced in α3L107Hβ2 compared with wild-type α3β2 (Fig. 5A) but not to the extent seen in wild-type α4β2. Our standard test concentration of 10 μM Oxa was only slightly inhibitory for α3L107Hβ2, but this behavior was considerably closer to that of α4 considering that Oxa substantially potentiates α3 responses at this concentration. A 5-fold higher Oxa concentration gave more α4-like inhibition, with a 4-fold decrease in potency and a significant increase in the Hill coefficient (Table 1). We also studied α3L107Cβ2, the cysteine substitution in this position

(Table 1). Its behavior on the whole was quite similar to that of wild-type α3β2, in particular maintaining potentiation by both Mor and Oxa; note the leftward-shifted EC_{50} values relative to ACh alone and E_{max} values >1.5. Although cysteine is polar and smaller than leucine, it does not introduce an aromatic group or the expected positive charge of the α4-based histidine substitution. After treatment with MTS reagents that introduce either a fixed positive charge or an imidazole group, currents evoked by ACh + Mor or ACh + Oxa in α3L107Cβ2 were reduced relative to controls, indicating that the position is accessible to the reagent and involved in modulation (L.C.C. and M.M.L., unpublished observations). Together, our results on the mutant α3L107Hβ2 and α3L107Cβ2 receptors strongly support a role of this position in modulation by Mor and Oxa.

In contrast to the α3Leu107 position, the mutation in position 113 (glutamate → arginine) showed marked discrimination between Mor and Oxa. Mor potentiation for α3E113Rβ2 was nearly identical to that of wild-type α3β2 (Fig. 5B; Table 1), although it had a slightly lower maximum effect at saturating agonist concentrations. However, Oxa effects were much more like wild-type α4β2, with a 2-fold rightward shift of EC_{50} and increased n_H relative to control. In addition, 10 μM Oxa inhibited ACh-evoked currents (side-by-side measurements; paired t test, $p < 0.05$) at all concentrations but the highest (3 mM).

The α3I117Tβ2 receptors had yet a third profile, with modulation by Mor and by Oxa much more like wild-type α4 than α3 receptors, without discriminating between the two (Fig. 5C; Table 1). Not only was Mor potentiation abolished for this receptor but also Mor inhibited at nonsaturating ACh concentrations. Likewise, similar to wild-type α4, Oxa inhibited most at lower ACh concentrations, shifting the response curve to the right with a 3-fold increase in EC_{50}.

We also studied three other positions in the α3 loop D and E regions. The best-fit parameters for these mutants are given in Table 1. The α3K109F substitution removes a positive charge and introduces an aromatic moiety. Despite this substantial change in physical character, Mor and Oxa still potentiated the ACh response to an extent similar to that of wild-type α3β2, if not better. The impact of another charge substitution—neutral and nonpolar to negatively charged—in the α3I57Eβ2 receptor was similar. Both Mor and Oxa potentiated the receptor with substantial 18-fold leftward shifts in EC_{50} for the concentration-response curve relative to ACh alone activation (compare 6-fold for wild-type α3β2). However, the overall improvement in efficacy in the presence of the modulator was less than that for the wild type, as indicated by E_{max} of 1.7 versus 2.6 for Mor and 1.2 versus 2.3 for Oxa. Finally, two mutations at position 115 of α3 gave rather surprising results. For substitutions of the α3 threonine with cysteine and with the α4-based glutamine, both Mor and Oxa still potentiated ACh-evoked responses; the leftward shift in EC_{50} (relative to ACh control) ranged from 13- to 125-fold. Although the relative efficacy of both modulators was approximately the same as wild-type α3β2 receptors for α3T115Cβ2 (a fairly conservative substitution), the E_{max} increased for both in the case of α3T115Qβ2. Along with our previous demonstration of substantial effects of MTS modification on Mor activity for α3T115Cβ2 (Seo et al., 2009), these results support a role of position 115 in modulation of these receptors. However, this position does not seem to discriminate between the two compounds.
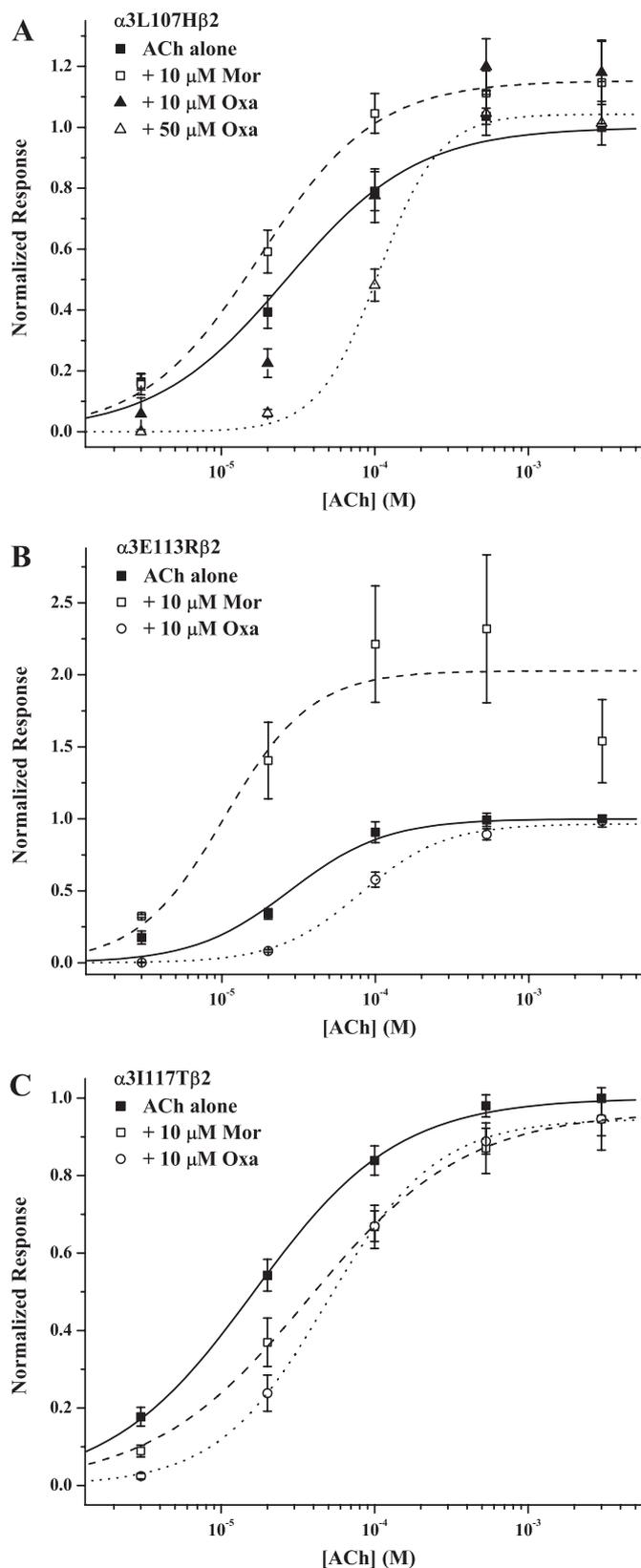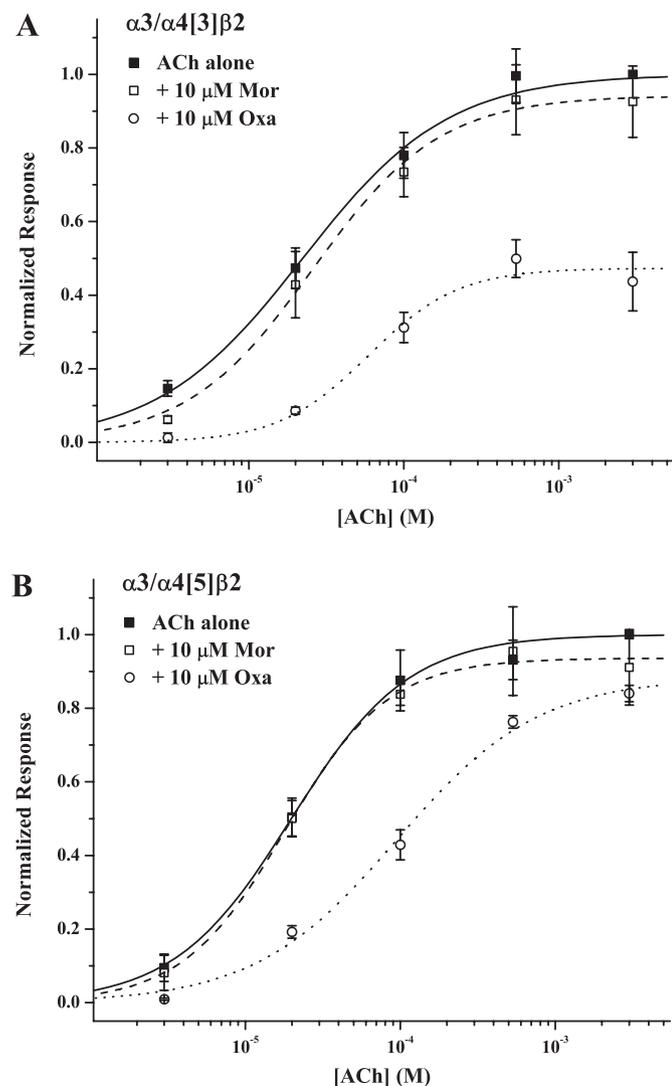
Fig. 5. α3 Single mutants reveal morantel and oxantel specificity. The three panels show concentration-response data for ACh-alone controls, in the presence of 10 μM Mor, and in the presence of 10 μM Oxa for the single-point mutants α3L107Hβ2 (A), α3E113Rβ2 (B), and α3I117Tβ2 (C). As described for the data in Fig. 4, the experiments with the two modulators were conducted separately, but the ACh control sets were analyzed in aggregate (per mutant). Symbols represent mean currents

normalized to 3 mM ACh alone (± S.E.M.), and fits of the Hill equation and numbers of replicates are reported in Table 1. The experiments were ■ and solid curves for ACh controls, □ and dashed curves for + Mor, and ○ and dotted curves for + Oxa (B and C) or ▲ (10 μM Oxa) and △ (50 μM Oxa) (A). For α3L107Hβ2, the dotted curve is the fit to the + 50 μM Oxa data set. The fit parameters for α3L107Hβ2 with 10 μM Oxa not reported elsewhere were EC_{50}, 63 ± 9 μM; n_H, 1.32 ± 0.20; E_{max}, 1.22 ± 0.04 (n = 6).

Not surprisingly, no single mutation that we studied converted α3 to α4 in terms of its modulation, so we next sought to generate α4-like modulation with combination mutants. To this end, we made α3/α4[3], the triple mutant α3L107H/E113R/I117T, and α3/α4[5], the quintuple mutant that adds α3T115Q and α3I57E to the triple mutant. Again we measured the effects of 10 μM Mor or 10 μM Oxa on the ACh concentration response for these mutant subtypes (Fig. 6). There were no apparent adverse effects of these mutations in combination on receptor function (for example, on protein folding or receptor assembly), as suggested by ACh-concentration-response behavior similar to that of the two wild-type receptors (Table 1) and by typical expression levels (evoked current magnitudes). In fact, the α3-based combination mutants interestingly had ACh responses very similar to those of wild-type α4β2, indicating an impact of this interface in channel activation (compare Seo et al., 2009). Both combination mutants also had Mor and Oxa modulation behavior more like that of α4 than of any of the single mutants but with some interesting differences (Table 1). The Mor-added condition gave ACh responses indistinguishable from those of control for the two combination mutants; that is, Mor did not potentiate these mutants. For the α3/α4[3] construct, the Oxa-added titration resulted in an EC_{50} shifted to lower potency (approximately 3-fold) and an efficacy much lower than control (E_{max} ~ 0.5); this efficacy was also lower than for Oxa inhibition of wild-type α4 receptors. Although the potency shift for the Oxa-added condition was larger at 4-fold for α3/α4[5], the efficacy was the same as in wild-type α4β2 receptors (E_{max} = 0.88) but, importantly, was less than control response.

To confirm that Oxa inhibits the α3 mutant receptors by the same mechanism as it does α4β2 receptors, we also studied the voltage-dependence of Oxa inhibition. These results are shown in Fig. 7A, which is a plot of the degree of inhibition as a function of holding potential. For the three point mutants showing the greatest α4-character (Fig. 5), we studied Oxa inhibition at two ACh concentrations. As was the case for wild-type α4β2, these data sets have effectively zero slopes. The only exception was the condition of 100 μM ACh for α3I117Tβ2 (△), which showed a shallow negative slope. We found similar results for the two combination mutants (data not shown in Fig. 7A for clarity). As was the case with Oxa inhibition of wild-type α4β2 receptors, these results are contrary to an open channel block mechanism.

Likewise, we confirmed that changing the subunit stoichiometry of α3-based receptors does not substantially alter Oxa inhibition. Figure 7B shows that Oxa inhibited indistinguishably receptors expressed by coinjecting the triple mutant α3/α4[3] and wild-type β2 RNAs in ratios of 10:1 and 1:10. As was the case with wild-type α4β2 receptors, different subunit stoichiometries do not seem to give rise to different modes of modulation by Mor and Oxa.

Fig. 6. Combination mutants have $\alpha4$ character. Concentration-response behavior for the two combination mutants are shown; $\alpha3/\alpha4[3]$ (A) is the triple mutant $\alpha3L107H/E113R/I117T$ and $\alpha3/\alpha4[5]$ (B) is the quintuple mutant $\alpha3I57E/L107H/E113R/T115Q/I117T$. Data were analyzed as described in Figs. 3 and 5 with the parameters for the fits reported in Table 1. The replicates were as follows: $n = 4$ (+ Mor, $\square$ and dashed curve), $n = 5$ (+ Oxa, $\bigcirc$ and dotted curve), and $n = 9$ (ACh controls, $\blacksquare$ and solid curve) for $\alpha3/\alpha4[3]$ (A); and $n = 4$ (+ Mor, $\square$ and dashed curve), $n = 6$ (+ Oxa, $\bigcirc$ and dotted curve), and $n = 10$ (ACh controls, $\blacksquare$ and solid curve) for $\alpha3/\alpha4[5]$ (B).

Discussion

We studied the effects of mutations at the noncanonical $\beta(+)/\alpha(-)$ interface on the allosteric modulation of neuronal nicotinic receptors by anthelmintic compounds. Our results support our previous hypothesis that this interface constitutes the modulator binding site, and we have identified several residues in the rat $\alpha3$ subunit that not only give rise to the subunit specificity for these compounds but also discriminate between Mor and Oxa. We have also unexpectedly discovered that modulation in this system can shift between the extremes of potentiation and inhibition with ostensibly minor structural changes in the receptor.

The Modulator Binding Site. Our data and previous reports in the literature support the conclusion that the $\beta(+)/\alpha(-)$ interface contains an allosteric modulator binding
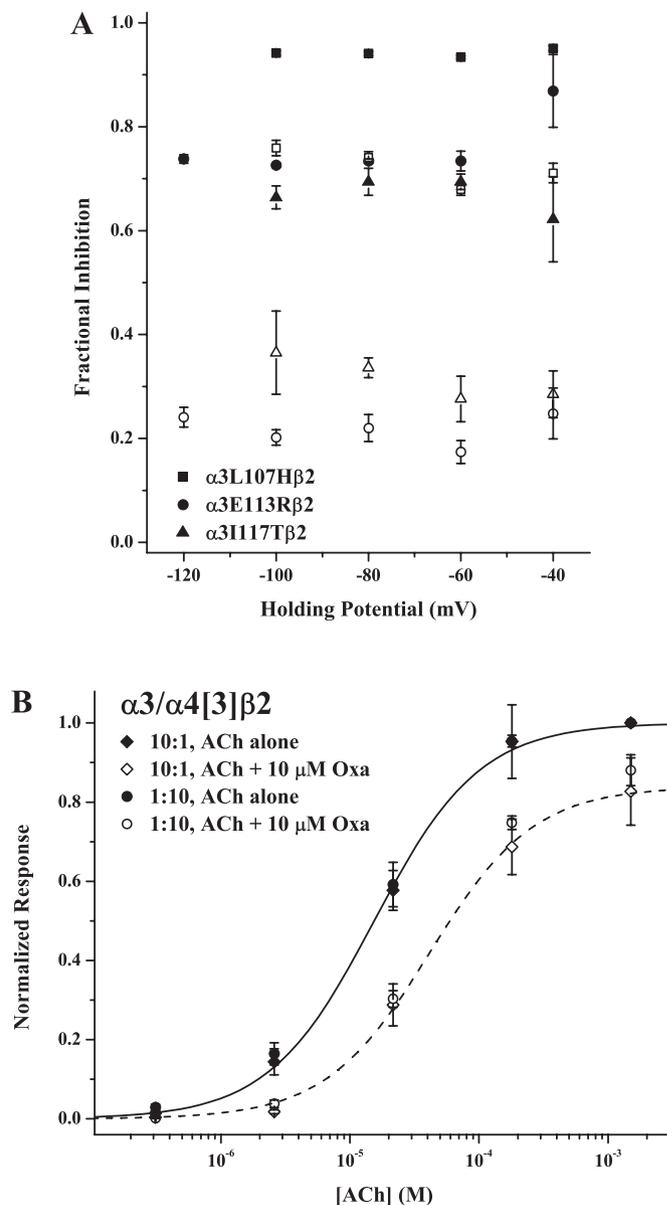
Fig. 7. Oxantel inhibition of $\alpha3$ mutants is noncompetitive and independent of subunit stoichiometry. A, the fractional degree of Oxa inhibition $[(I_{ACh} - I_{ACh+Oxa})/I_{ACh}]$ is plotted versus holding potential for three point mutants ($\alpha3L107H\beta2$, squares; $\alpha3E113R\beta2$, circles; $\alpha3I117T\beta2$, triangles). In all cases, the filled and open symbols represent the lower (20 μM) and higher (100 μM) ACh concentrations, respectively. Control and Oxa coapplied responses at each ACh concentration were recorded on the same set of oocytes; the Oxa concentration was 10 μM for $\alpha3E113R\beta2$ and $\alpha3I117T\beta2$ and 50 μM for $\alpha3L107H\beta2$. Symbols represent means ($\pm$ S.E.M.) for $n = 3$ or 4; in some cases, error bars are smaller than the symbol. B, the effect of subunit stoichiometry on Oxa inhibition of the triple mutant $\alpha3/\alpha4[5]\beta2$ is shown. Responses evoked by ACh alone are shown as $\blacklozenge$ (10:1 RNA injection ratio) and $\bullet$ (1:10), whereas responses to ACh + 10 μM Oxa are given as $\lozenge$ (10:1) and $\bigcirc$ (1:10). All currents were normalized to the response to 1.5 mM ACh alone; values plotted are means $\pm$ S.E.M. For clarity, fits of the Hill equation to only the 10:1 ratio data are shown, with the solid curve for the ACh alone responses and the dashed curve for the Oxa inhibition case. The parameters of the Oxa inhibition, not reported elsewhere, were EC$_{50}$, 42 $\pm$ 13 μM; n_H, 1.08 $\pm$ 0.29; E_{max}, 0.84 $\pm$ 0.07 (10:1 ratio) and EC$_{50}$, 40 $\pm$ 5 μM; n_H, 1.09 $\pm$ 0.11; E_{max}, 0.90 $\pm$ 0.03 (1:10 ratio). The parameters for the control ACh responses were EC$_{50}$, 14 $\pm$ 1 μM; n_H, 1.01 $\pm$ 0.09 (10:1 ratio) and EC$_{50}$, 15 $\pm$ 2 μM; n_H, 1.06 $\pm$ 0.17 (1:10 ratio). The replicates were $n = 5$ for each experiment.

site. As shown in Fig. 3 and Table 1, mutation of the two highly conserved tryptophans to alanine (α3W53A and β2W149A) abolished the potentiation by Mor and Oxa seen in wild-type α3β2. Although it is tempting to interpret these results as substantially reducing modulator affinity (thereby supporting a direct role in binding), the effects are no doubt more complicated (for example, the 2.5-fold increase in EC_{50} for ACh activation and $E_{max} = 0.90$ in the presence of Oxa indicate inhibition).

We demonstrated previously that residues in this interface, particularly β2Thr150 and α3Thr115, contribute to allosteric potentiation (Seo et al., 2009). The gross structural homology of this interface pocket to the canonical agonist site and the fact that four of the five residues of the "aromatic box" are conserved further substantiate this as a ligand binding site. In addition, Hsiao et al. (2006) and Moroni et al. (2008) found that residues in this same vicinity of noncanonical interfaces in neuronal nAChRs are responsible for modulation by divalent cations.

Furthermore, the modulation of nAChRs by anthelmintic compounds parallels that of GABA$_A$ receptors by benzodiazepines, the noncanonical interface binding sites of which are well established (e.g., Miller and Smart, 2010). For example, radioligand binding assays, evoked-current measurements, and chemical modification experiments for receptors with mutations in these positions indicate that γ2Thr81, γ2Arg132, and γ2Thr142 play roles in benzodiazepine/hypnotic binding or modulation (Kucken et al., 2000; Teissére and Czajkowski, 2001; Hanson et al., 2008). These residues are homologous to the α3Ile57, α3Leu107, and α3Ile117 nAChR residues, respectively, found to govern Mor and Oxa activities (Figs. 5 and 6; Table 1). Although it is possible that Mor and Oxa bind elsewhere to the nicotinic receptor, all our results are consistent with a binding site at the β(+)/α(−) interface. This demonstration suggests that five (potential) interface ligand binding sites are a general feature of the Cys-loop receptor superfamily.

Specificity of Modulation. The major goal of this study was to understand the specificity of modulator-binding site interactions. Our limited structure-activity relationship design, exploring both the compounds and subunits, yielded specificity information about both. Five of the six positions differing between α3 and α4 that we studied (Fig. 4) had essentially parallel effects on Mor and Oxa activity, suggesting little ability to discriminate between the two. In contrast, α3E113Rβ2 showed unambiguous differences for the two compounds.

The positions α3Ile57 and α3Thr115, although involved in modulation, do not seem to affect modulation specificity. α3I57Eβ2 receptors were clearly still potentiated by Mor and Oxa, given the leftward-shifted EC_{50} values, but the E_{max} values were lower than for wild-type α3β2 (Table 1). The conservative cysteine and the α4-based glutamine substitutions for α3Thr115 gave receptors that were potentiated substantially ($E_{max} > 1$ and leftward-shifted EC_{50}) by both Mor and Oxa (Table 1; see also Seo et al., 2009). However, α3T115Qβ2 was potentiated better than wild-type α3β2, judging by the elevation in E_{max} and the degree of the EC_{50} shift. In contrast, the α3K109Fβ2 receptor displayed Mor and Oxa potentiation very similar to that of wild-type α3β2 (Table 1) and may play no role in modulation by these compounds. Both α3Ile57 and α3Thr115 are probably closer to the two tryptophans than α3Lys109 (Fig. 4).

Mutations in positions α3Leu107 and α3Ile117 were similar in giving more α4-like modulation than the aforementioned mutants. Both α3L107Hβ2 and α3I117Tβ2 receptors lost Mor potentiation and exhibited partial inhibition by Oxa (Fig. 5; Table 1), but neither Mor nor Oxa distinguished between the two compounds to any large degree. It is noteworthy that the α3L107Cβ2 mutant was modulated similarly to wild-type α3β2, implicating positive charge and/or aromaticity at this location for inhibition.

Mutation of α3Glu113 also led to inhibition, but only by Oxa (Fig. 5; Table 1). The leftward-shifted EC_{50} and E_{max} ~2 in the presence of Mor demonstrate clear potentiation, whereas the rightward-shifted EC_{50} and E_{max} ~1 with Oxa signify inhibition. These results indicate either that Oxa contacts α3Glu113 whereas Mor does not, or that Oxa and Mor interact differently with this residue. Compared with positions α3Ile57, α3Lys109, and α3Thr115, the residues α3Leu107, α3Glu113, and α3Ile117 seem to be dominant in dictating inhibition as the mode of modulation, because Oxa inhibition was more pronounced for the triple mutant than for the quintuple mutant or wild-type α4β2 receptors (Fig. 6).

Bartos et al. (2006, 2009) have studied the differences in pharmacological activity of these same anthelmintics on mammalian muscle-type and α7 receptors. They found that α7Gln57 was important for specificity of morantel, but not oxantel (Bartos et al., 2009); this position is homologous to α3Lys55, which is identical in α4 (Fig. 4). Nonetheless, their results are consistent with our finding of the importance of the complementary face, D loop residues for the activity of these anthelmintics. Because these compounds are full or partial agonists, acting at canonical sites, of α7 and muscle-type nAChRs (Bartos et al., 2009), an interesting question arises regarding the specificity differences between canonical and noncanonical sites. Although there are other differences between α3 and α4 in these loop D and E equivalents, and we may not have completely delimited the anthelmintic modulator binding site, the residues we identified account for the majority of the α4-like responses to Mor and Oxa, as indicated by the combination mutants (Fig. 6).

Switching the Modulation Mechanism. How can we explain our findings in a comprehensive way, especially in regard to a mechanistic switch between potentiation and inhibition? Noncanonical interfaces govern modulation of α4-containing receptors by divalent cations, but whether the modulation is inhibition or potentiation seems to depend on the receptor stoichiometry (Hsiao et al., 2006; Moroni et al., 2008). In our studies, altering the ratio of injected subunit RNAs did not change Oxa inhibition substantially for either wild-type or mutant receptors (Figs. 2 and 7). This suggests that differential subunit stoichiometry selectivity cannot explain the differences in Mor and Oxa modulation, which is consistent with our general conclusion that Mor/Oxa modulation requires both α and β subunits.

We demonstrated previously that Mor potentiates α3β2 by enhancing gating efficacy, probably by increasing the rate of channel opening (Wu et al., 2008), similar to the finding that zinc enhances α4 channel open probability through increased burst duration (Hsiao et al., 2008). In other words, a Mor-bound receptor favors the open state of the channel preferentially over the closed state, relative to the control of activation by ACh alone. We are intrigued by an observation for all the mutants in the current study that the shift in EC_{50}

and E_{max} in the presence of Mor or Oxa were each correlated with the shift in EC_{50} for ACh activation relative to wild-type $\alpha3\beta2$. For example, the mutations $\alpha3I57E$ and $\alpha3T115Q$ reduced ACh potency, and potentiation was greater than for the wild-type $\alpha3\beta2$ receptor, whereas $\alpha3L107H$, $\alpha3I117T$, and the triple and quintuple combinations increased ACh potency, and potentiation was greatly reduced or inhibition obtained (Table 1). If the modulator, when bound, establishes approximately the same closed $\leftrightarrow$ open equilibrium independent of other factors, then inhibition (which we found to be noncompetitive; Figs. 2 and 7) is merely a decrease in efficacy relative to control. Further work is required to substantiate this mechanism, for example, by finding mutations in this region of $\alpha3$ that would yield definitive Mor inhibition, as well as recording single-channel activity to measure efficacy directly.

Our work indicates that adjacent residues can favor either the closed or open state of the receptor and that such residues are located in the complementary $(-)$ side of binding site interfaces. In light of previous studies, neither of these ideas is surprising. Collins and Millar (2010) demonstrated that mutations clustered in the transmembrane domain of $\alpha7$ receptors could convert potentiation by ivermectin into inhibition. Likewise, many studies support a role of the complementary face of the canonical binding site in channel activation (e.g., Mukhtasimova and Sine, 2007; Young et al., 2007). That such apparently important contributions to gating arise in the noncanonical interfaces (our work) raises questions about the symmetry requirements of activation for nAChRs (compare Rayes et al., 2009). Likewise, mapping the spatial distribution of residues promoting channel opening versus closing in this region may help illuminate how subunits move in converting between these conformations (Corringer et al., 2010). In addition to these issues fundamental to ion channel function, our work suggests a very specific region of $\alpha3$ and $\alpha4$ nAChRs to target for drug design.

Acknowledgments

Authorship Contributions

Participated in research design: Cesa, Higgins, Sando, Kuo, and Levandoski.

Conducted experiments: Cesa, Higgins, Sando, Kuo, and Levandoski.

Contributed new reagents or analytic tools: Cesa, Higgins, Sando, Kuo, and Levandoski.

Performed data analysis: Cesa, Higgins, Sando, Kuo, and Levandoski.

Wrote or contributed to the writing of the manuscript: Cesa, Higgins, Sando, Kuo, and Levandoski.

References

Albuquerque EX, Pereira EF, Alkondon M, and Rogers SW (2009) Mammalian nicotinic acetylcholine receptors: from structure to function. *Physiol Rev* **89:**73–120.

Arias HR (2000) Localization of agonist and competitive antagonist binding sites on nicotinic acetylcholine receptors. *Neurochem Int* **36:**595–645.

Arias HR, Bhumireddy P, and Bouzat C (2006) Molecular mechanisms and binding site locations for noncompetitive antagonists of nicotinic acetylcholine receptors. *Int J Biochem Cell Biol* **38:**1254–1276.

Bartos M, Rayes D, and Bouzat C (2006) Molecular determinants of pyrantel selectivity in nicotinic receptors. *Mol Pharmacol* **70:**1307–1318.

Bartos M, Price KL, Lummis SC, and Bouzat C (2009) Glutamine 57 at the complementary binding-site face is a key determinant of morantel selectivity for $\alpha7$ nicotinic receptors. *J Biol Chem* **284:**21478–21487.

Bertrand D and Gopalakrishnan M (2007) Allosteric modulation of nicotinic acetylcholine receptors. *Biochem Pharmacol* **74:**1155–1163.

Birks J (2006) Cholinesterase inhibitors for Alzheimer's disease. *Cochrane Database Syst Rev* (**1**):CD005593.

Boulter J, Connolly J, Deneris E, Goldman D, Heinemann S, and Patrick J (1987) Functional expression of two neuronal nicotinic acetylcholine receptors from cDNA clones identifies a gene family. *Proc Natl Acad Sci USA* **84:**7763–7767.

Brejc K, van Dijk WJ, Klaassen RV, Schuurmans M, van Der Oost J, Smit AB, and Sixma TK (2001) Crystal structure of an ACh-binding protein reveals the ligand-binding domain of nicotinic receptors. *Nature* **411:**269–276.

Broad LM, Zwart R, Pearson KH, Lee M, Wallace L, McPhie GI, Emkey R, Hollinshead SP, Dell CP, Baker SR, et al. (2006) Identification and pharmacological profile of a new class of selective nicotinic acetylcholine receptor potentiators. *J Pharmacol Exp Ther* **318:**1108–1117.

Buisson B and Bertrand D (1998) Open-channel blockers at the human $\alpha4\beta2$ neuronal nicotinic receptor. *Mol Pharmacol* **53:**555–563.

Cohen BN, Figl A, Quick MW, Labarca C, Davidson N, and Lester HA (1995) Regions of $\beta2$ and $\beta4$ responsible for differences between the steady state dose-response relationships of the $\alpha3\beta2$ and $\alpha3\beta4$ neuronal nicotinic receptors. *J Gen Physiol* **105:**745–764.

Collins T and Millar NS (2010) Nicotinic acetylcholine receptor transmembrane mutations convert ivermectin from a positive to a negative allosteric modulator. *Mol Pharmacol* **78:**198–204.

Colquhoun D (1998) Binding, gating, affinity and efficacy: the interpretation of structure-activity relationships for agonists and of the effects of mutating receptors. *Br J Pharmacol* **125:**924–947.

Corringer PJ, Baaden M, Bocquet N, Delarue M, Dufresne V, Nury H, Prevost M, and Van Renterghem C (2010) Atomic structure and dynamics of pentameric ligand-gated ion channels: new insight from bacterial homologues. *J Physiol* **588:**565–572.

Dani JA and Bertrand D (2007) Nicotinic acetylcholine receptors and nicotinic cholinergic mechanisms of the central nervous system. *Annu Rev Pharmacol Toxicol* **47:**699–729.

Gonzales D, Rennard SI, Nides M, Oncken C, Azoulay S, Billing CB, Watsky EJ, Gong J, Williams KE, Reeves KR, et al. (2006) Varenicline, an alpha4beta2 nicotinic acetylcholine receptor partial agonist, vs sustained-release bupropion and placebo for smoking cessation: a randomized controlled trial. *JAMA* **296:**47–55.

Gotti C, Clementi F, Fornari A, Gaimarri A, Guiducci S, Manfredi I, Moretti M, Pedrazzi P, Pucci L, and Zoli M (2009) Structural and functional diversity of native brain neuronal nicotinic receptors. *Biochem Pharmacol* **78:**703–711.

Hanson SM, Morlock EV, Satyshur KA, and Czajkowski C (2008) Structural requirements for eszopiclone and zolpidem binding to the γ-aminobutyric acid type-A (GABA$_A$) receptor are different. *J Med Chem* **51:**7243–7252.

Harpsøe K, Ahring PK, Christensen JK, Jensen ML, Peters D, and Balle T (2011) Unraveling the high- and low-sensitivity agonist responses of nicotinic acetylcholine receptors. *J Neurosci* **31:**10759–10766.

Henderson BJ, Pavlovicz RE, Allen JD, González-Cestari TF, Orac CM, Bonnell AB, Zhu MX, Boyd RT, Li C, Bergmeier SC, et al. (2010) Negative allosteric modulators that target human $\alpha4\beta2$ neuronal nicotinic receptors. *J Pharmacol Exp Ther* **334:**761–774.

Hsiao B, Mihalak KB, Repicky SE, Everhart D, Mederos AH, Malhotra A, and Luetje CW (2006) Determinants of zinc potentiation on the $\alpha4$ subunit of neuronal nicotinic receptors. *Mol Pharmacol* **69:**27–36.

Hsiao B, Mihalak KB, Magleby KL, and Luetje CW (2008) Zinc potentiates neuronal nicotinic receptors by increasing burst duration. *J Neurophysiol* **99:**999–1007.

Hurst RS, Hajós M, Raggenbass M, Wall TM, Higdon NR, Lawson JA, Rutherford-Root KL, Berkenpas MB, Hoffmann WE, Piotrowski DW, et al. (2005) A novel allosteric modulator of the $\alpha7$ neuronal nicotinic acetylcholine receptor: in vitro and in vivo characterization. *J Neurosci* **25:**4396–4405.

Jensen AA, Frølund B, Liljefors T, and Krogsgaard-Larsen P (2005) Neuronal nicotinic acetylcholine receptors: structural revelations, target identifications, and therapeutic inspirations. *J Med Chem* **48:**4705–4745.

Karlin A and Akabas MH (1998) Substituted-cysteine accessibility method. *Methods Enzymol* **293:**123–145.

Krause RM, Buisson B, Bertrand S, Corringer PJ, Galzi JL, Changeux JP, and Bertrand D (1998) Ivermectin: a positive allosteric effector of the $\alpha7$ neuronal nicotinic acetylcholine receptor. *Mol Pharmacol* **53:**283–294.

Kucken AM, Wagner DA, Ward PR, Teissére JA, Boileau AJ, and Czajkowski C (2000) Identification of benzodiazepine binding site residues in the $\gamma2$ subunit of the γ-aminobutyric acid A receptor. *Mol Pharmacol* **57:**932–939.

Maelicke A and Albuquerque EX (2000) Allosteric modulation of nicotinic acetylcholine receptors as a treatment strategy for Alzheimer's disease. *Eur J Pharmacol* **393:**165–170.

Mazzaferro S, Benallegue N, Carbone A, Gasparri F, Vijayan R, Biggin PC, Moroni M, and Bermudez I (2011) Additional acetylcholine (ACh) binding site at $\alpha4/\alpha4$ interface of $(\alpha4\beta2)_2\alpha4$ nicotinic receptor influences agonist sensitivity. *J Biol Chem* **286:**31043–31054.

Miller PS and Smart TG (2010) Binding, activation and modulation of Cys-loop receptors. *Trends Pharmacol Sci* **31:**161–174.

Moroni M, Vijayan R, Carbone A, Zwart R, Biggin PC, and Bermudez I (2008) Non-agonist-binding subunit interfaces confer distinct functional signatures to the alternate stoichiometries of the $\alpha4\beta2$ nicotinic receptor: an $\alpha4$-$\alpha4$ interface is required for Zn^{2+} potentiation. *J Neurosci* **28:**6884–6894.

Mukhtasimova N and Sine SM (2007) An intersubunit trigger of channel gating in the muscle nicotinic receptor. *J Neurosci* **27:**4110–4119.

Nirthanan S, Garcia G 3rd, Chiara DC, Husain SS, and Cohen JB (2008) Identifi-

cation of binding sites in the nicotinic acetylcholine receptor for TDBzl-etomidate, a photoreactive positive allosteric effector. *J Biol Chem* **283:**22051–22062.

Rang HP (1981) Drugs and ionic channels: mechanism and implications. *Postgrad Med J* **57:**89–97.

Rayes D, De Rosa MJ, Sine SM, and Bouzat C (2009) Number and locations of agonist binding sites required to activate homomeric Cys-loop receptors. *J Neurosci* **29:**6022–6032.

Rucktooa P, Smit AB, and Sixma TK (2009) Insight in nAChR subtype selectivity from AChBP crystal structures. *Biochem Pharmacol* **78:**777–787.

Sallette J, Bohler S, Benoit P, Soudant M, Pons S, Le Novère N, Changeux JP, and Corringer PJ (2004) An extracellular protein microdomain controls up-regulation of neuronal nicotinic acetylcholine receptors by nicotine. *J Biol Chem* **279:**18767–18775.

Schrattenholz A, Pereira EF, Roth U, Weber KH, Albuquerque EX, and Maelicke A (1996) Agonist responses of neuronal nicotinic acetylcholine receptors are potentiated by a novel class of allosterically acting ligands. *Mol Pharmacol* **49:**1–6.

Seo S, Henry JT, Lewis AH, Wang N, and Levandoski MM (2009) The positive allosteric modulator morantel binds at noncanonical subunit interfaces of neuronal nicotinic acetylcholine receptors. *J Neurosci* **29:**8734–8742.

Sine SM and Engel AG (2006) Recent advances in Cys-loop receptor structure and function. *Nature* **440:**448–455.

Teissére JA and Czajkowski C (2001) A β-strand in the γ2 subunit lines the benzodiazepine binding site of the GABA$_A$ receptor: structural rearrangements detected during channel gating. *J Neurosci* **21:**4977–4986.

Wu TY, Smith CM, Sine SM, and Levandoski MM (2008) Morantel allosterically enhances channel gating of neuronal nicotinic acetylcholine α3β2 receptors. *Mol Pharmacol* **74:**466–475.

Young GT, Broad LM, Zwart R, Astles PC, Bodkin M, Sher E, and Millar NS (2007) Species selectivity of a nicotinic acetylcholine receptor agonist is conferred by two adjacent extracellular β4 amino acids that are implicated in the coupling of binding to channel gating. *Mol Pharmacol* **71:**389–397.

Zwart R and Vijverberg HP (1998) Four pharmacologically distinct subtypes of α4β2 nicotinic acetylcholine receptor expressed in *Xenopus laevis* oocytes. *Mol Pharmacol* **54:**1124–1131.

Address correspondence to: Mark Levandoski, Department of Chemistry, 1116 8th Avenue Grinnell, IA 50112. E-mail: levandos@grinnell.edu